05 Oct 2023

# Improving Rheological And Thermal Performance Of Gilsonite-Modified Binder With Phase Change Materials

Farshad Saberi K.

Yizhuang David Wang

Jenny Liu
*Missouri University of Science and Technology*, jennyliu@mst.edu



## Recommended Citation

F. Saberi K. et al., "Improving Rheological And Thermal Performance Of Gilsonite-Modified Binder With Phase Change Materials," *Construction and Building Materials*, vol. 399, article no. 132557, Elsevier, Oct 2023.
The definitive version is available at https://doi.org/10.1016/j.conbuildmat.2023.132557

Construction and Building Materials 399 (2023) 132557

Contents lists available at ScienceDirect

Construction and Building Materials

journal homepage: www.elsevier.com/locate/conbuildmat

# Improving rheological and thermal performance of Gilsonite-Modified binder with phase change materials

Farshad Saberi K., Yizhuang David Wang, Jenny Liu *

*Department of Civil, Architectural and Environmental Engineering, Missouri University of Science and Technology, Rolla, MO 65409, United States*

ARTICLE INFO

*Keywords:*
Gilsonite
Phase change material
PEG
Thermal properties
Rheological properties
Fatigue
Low-temperature performance

ABSTRACT

Gilsonite, as a type of natural asphalt binder, has been used to improve the high-temperature performance of regular asphalt binders. However, the addition of gilsonite may compromise binders' low-temperature thermal cracking resistance. In this research, polyethylene glycol (PEG), as one type of the phase change materials (PCMs), was used as an innovative material to balance the impacts of gilsonite on high and low performance of asphalt binders. The dosages of gilsonite and PEG were first determined based on the materials' rheological behaviors at low temperatures. The performance of the PEG-gilsonite-modified binder was then fully evaluated in terms of the resistance to cracking and rutting at various temperatures. Thermal tests were also conducted to assess the thermal behaviors of the modified binders. The testing results indicate that with the proper dosage of gilsonite and PEG, the rutting resistance of the binder can be improved without sacrificing its low-temperature performance. With the addition of the PCM, the binder was tested to have high volumetric heat capacity, which indicates PCM can reduce the rate and the magnitude of the temperature changes in pavements.

## 1. Introduction

Gilsonite is a naturally occurring glossy black asphaltic and known as asphalt binder modifier for its good affinity with asphalt and superior bonding. As a natural lake asphalt, gilsonite can be quickly dissolved in the binder and coat aggregate particles during the mixing process providing additional bonding strength between different components. In a previous research study, the researchers have found that using gilsonite-modified binders can improve stripping resistance of pavements and reduce the shoving and rutting susceptibility [1]. Kok et al. confirmed that as the dosage of gilsonite increased, the value of the rutting parameter ($G^*/\sin\delta$) increased, indicating the rutting resistance was improved. The findings have been confirmed by other researchers using testing methods such as the multiple-stress creep- recovery (MSCR) test [2–6]. However, it has also been reported that incorporating gilsonite may adversely affect the fatigue and low-temperature performance of pavements as it changes the oil-to-asphaltene content ([4,5,7–9]). The addition of gilsonite can also increase the mixing and compaction temperatures as the gilsonite increases the binder viscosity; thus, leading to greater energy consumption [10].

Phase-change materials (PCMs), on the other hand, have been used in civil infrastructures to regulate dramatic temperature changes and improve the thermal behaviors of construction materials, respecting their high latent thermal storage capacity. PCM can absorb and release a great amount of energy during the phase transition between solid–solid, solid–liquid or solid–gas at specific temperature range [11]. For example, PCM has been incorporated in Portland cement concrete and considered as a novel technology to reduce energy usage and keep the temperature of building interior spaces at the comfortable zone [12]. Engineers have also used PCM in paving concrete to store energy and function as a heat source to melt ice/ snow in pavements [13].

Besides regulating temperatures, PCM with low melting points have been incorporated into asphalt binder to improve the low-temperature performance of binders. The low-temperature stiffness of asphalt binder has been found to be correlated to its glass transition temperature. Binders with lower glass transition temperature usually are softer at low temperatures; thus, experiencing less intense thermal stress when temperature decreases [14]. Moreover, the glass transition temperature is a function of the molecular weight of the material [15]. Therefore, lowering the molecular weight of the asphalt binder can effectively decrease the glass transition temperature; thus, improving the low-temperature performance.

On the other hand, PCM with low melting point is usually associated with low molecular weight. For instance, PCM with a melting point of

* Corresponding author.
*E-mail addresses:* farshad@mst.edu (F. Saberi K.), y.wang@mst.edu (Y.D. Wang), jennyliu@mst.edu (J. Liu).

https://doi.org/10.1016/j.conbuildmat.2023.132557
Received 3 November 2022; Received in revised form 12 June 2023; Accepted 17 July 2023
Available online 24 July 2023

**Table 1**
Basic Characteristics of Polyethylene Glycol.

| Physical properties | Values or characteristics |
|---|---|
| Molecular weight (g.mol$^{-1}$) | 400 |
| Physical state | Liquid |
| Flash point (°C) | 235 |
| Specific gravity | 1.128 |
| Viscosity (mPa·s at 20 °C) | 110–125 |
| Solubility | Soluble in water |
| Melting Point (°C) | 4.0 |

**Table 2**
Gilsonite Specification and Properties.

| Physical properties | Measured values |
|---|---|
| Penetration | 0 |
| Softening point (°C) | 160–185 |
| Flash point (°C) | 316 |
| Specific gravity | 1.06 |
| Ash | ≤1.0% |
| Decomposition temperature (°C) | 287.8 |

4 °C has a molecular weight of 400 g/mol. The molecular weight of PCM is lower compared to the average molecular weights of the four fractions of asphalt binder, i.e., saturates, aromatics, resins, and asphaltenes, which are 566, 630, 888, and 1937 g/mol, respectively. Therefore, incorporating PCM with a low melting point into asphalt binder has been considered as a measure to the binder low-temperature cracking resistance [15,16]. Kakar et al. employed microencapsulated PCM with Tetradecane and the melting point of 6 °C in two different dosages, i.e., 1%, and 3% by weight. The temperature sweep test indicated adding PCM decreased the complex modulus at different temperatures for binder [17]. Polyurethane solid–solid phase change material (PUSSPCM) with low phase change temperature was utilized in asphalt binder by a direct incorporation method at different percentages, i.e., 0, 3, 5, and 7% by weight. The results showed polyurethane solid–solid PCM had slightly improved the high-temperature rutting performance but induced a significant decrease in creep stiffness, which was a great improvement in low temperature performance [18].

In this study, gilsonite and a polyethylene glycol (PEG) which is a latent heat storage PCM with a low melting point were used as asphalt binder modifiers to improve the binder performance under a large range of temperatures. In the previous study, gilsonite was found to be able to improve the binder rutting resistance while compromising the low-temperature cracking resistance [1]. The objective of this study is to identify the proper dosages of gilsonite and PCM that increase the high-temperature rutting resistance without compromising the binder low-temperature performance. A series of rheological tests were conducted to evaluate the behaviors of the gilsonite-PEG-modified binder at high, low, and intermediate temperatures. Thermal tests were performed to assess the impact of the additives on the thermal properties of the binders.

## 2. Materials and specimen preparation

### 2.1. Materials

An Alaskan PG 52–28 binder was used as the base binder in this study. A U.S. manufactured gilsonite was selected as the binder modifier to enhance the high-temperature performance. The gilsonite was in powder form before mixed with the base binder. A PEG with an average molar mass of 400 g·mol$^{-1}$ (PEG 400) and a low melting point of 4 °C was added to ensure the binder's low-temperature performance. The testing results from the preliminary study suggested that when over 5% of PEG was mixed with binder, segregation between PEG and binder started to occur. Therefore, the dosage of PEG 400 was limited to 5%.

**Table 3**
Modified Binders with Different Dosages of Gilsonite and PEG.

| Designation | Polyethylene glycol (%) | Gilsonite (%) |
|---|---|---|
| Neat binder | 0 | 0 |
| G3 | 0 | 3 |
| G6 | 0 | 6 |
| G9 | 0 | 9 |
| G12 | 0 | 12 |
| P5G3 | 5 | 3 |
| P5G6 | 5 | 6 |
| P5G9 | 5 | 9 |
| P5G12 | 5 | 12 |

**Table 4**
Summary of Binder Tests.

| Test | Purpose | Parameter | Specification |
|---|---|---|---|
| Rotational viscometer test | Mixing and compaction temperature | $\eta$ | AASHTO T 316 |
| Bending beam rheometer | Low temperature performance | $S$, $m$-$value$, $\Delta T_c$ | AASHTO T 313 |
| Dynamic shear rheometer (DSR) test | High temperature performance grade | $G^*/\sin\delta$ | AASHTO M 320 |
| Multiple Stress Creep Recovery (MSCR) test | High temperature performance | $J_{nr}$ and $R$ | AASHTO T 350 |
| Glover-Rowe (G-R) parameter analysis | Cracking potential | $G$-$R$ | Not Applicable |
| Linear amplitude sweep (LAS) test | Fatigue resistance | C-S curve, $N_f$ | AASHTO T 391 |
| Thermal conductivity and heat capacity test | Thermal conductivity and heat capacity test | $k$, $c$ | Not Applicable |
| Thermogravimetric Analysis (TGA) | Degradation temperature | $T$ | Not Applicable |
| Differential Scanning Calorimetry (DSC) Test | Glass transition temperature | $T_g$ | Not Applicable |

Table 1 presents the physical and thermal properties of PEG 400, and the properties of gilsonite are presented in Table 2.

### 2.2. Preparation of PEG and gilsonite-modified asphalt binders

The mixing temperature to blend the base binder and the additives was determined to be 185 °C based on the softening point of gilsonite. The neat binder was first heated to the target temperature in a heating mantle. The gilsonite powder was added gradually to the binder to ensure a uniform dispersion. The mixture was stirred for 30 min using a high shear mixer at 2000 rpm. PEG 400 was added afterwards and mixed for another 30 min at 4000 rpm. To limit the evaporation and decomposition of PEG, the heating temperature was decreased to 150 °C before the addition of PEG. Different dosages of gilsonite were used in this study, and the samples were designated based on the percentages of the modifiers. For example, P5G6 indicated the binder contained 5% PEG and 6% gilsonite by weight. Table 3 presents the designations of the modified binders, types of modifiers, and the percentages used in this research.

## 3. Research methods

In this study, the performance of the modified asphalt binders was evaluated through rheological tests at different temperatures targeting different types of distresses. The tests included dynamic shear modulus test, the bending beam rheometer (BBR) test, the multiple stress creep recovery (MSCR) test, and the linear amplitude sweep (LAS) test. The binders with different dosages of modifiers were graded based on the Superpave performance grading system, and the testing results were analyzed by the performance models and parameters such as $\Delta T_c$, the Glover-Rowe (G-R) parameter, and the ViscoElastic Continuum Damage

(VECD) model. Thermal tests and analyses were conducted following the rheological tests to evaluate the impact of the PCM on asphalt binder thermal behaviors. The thermal conductivity, heat capacity, and glass transition temperatures of the modified binders were measured, the decomposition temperature was evaluated using thermogravimetric analysis (TGA) methods. The testing methods and the corresponding evaluation parameters in this study are summarized in Table 4.

### 3.1. Tests for binder viscosity and workability

The viscosity of the binders was measured using the rotational viscometer (RV) at 125, 135, 145, and 155 °C. The RV test was conducted to evaluate the pumpability, mixability, and workability of the binder. The test was also used to determine the mixing and compaction temperatures for different binders.

### 3.2. Low-Temperature tests for cracking susceptibility evaluation

The BBR test was used to determine the low-temperature performance grades (PGs) of the binders. The tests were conducted at −12, −18, and −24 °C after the Rolling Thin-Film Oven (RTFO) and Pressure Aging Vessel (PAV) aging conditioning. In addition to using the low performance grade, the cracking resistance of the modified binders at low temperatures were also evaluated using the $\Delta T_c$ parameter. The parameter was obtained by calculating the difference between the critical temperatures for creep stiffness ($T_{c,S}$) and relaxation rate ($T_{c,m}$). The critical temperatures were determined using Eqs. (1) and (2).

$$T_{c,S} = T_1 + \left(\frac{(T_1 - T_2) \times (\log 300 - \log S_1)}{\log S_1 - \log S_2}\right) - 10 \quad (1)$$

$$T_{c,m} = T_1 + \left(\frac{(T_1 - T_2) \times (0.300 - m_1)}{m_1 - m_2}\right) - 10 \quad (2)$$

where, $S_1$ is the creep stiffness at $T_1$ in MPa, $S_2$ is the creep stiffness at $T_2$ in MPa, $m_1$ is the creep rate at $T_1$, $T_1$ is the temperature (°C) at which $S$ and $m$ pass the criteria ($S \leq 300$ MPa and $m \geq 0.300$), and $T_2$ is the temperature (°C) at which S and m no longer meet the criteria (S>300 MPa or m<0.300). The $\Delta Tc$ value was then calculated using Eq. (3).

$$\Delta T_c = T_{c,S} - T_{c,m} \quad (3)$$

### 3.3. High-Temperature tests for rutting resistance evaluation

In terms of rutting resistance, the binders were evaluated using the Superpave rutting factor ($G^*/\sin\delta$) and the MSCR test. Both tests were conducted on a dynamic shear rheometer (DSR). The rutting factor, $G^*/\sin\delta$, was obtained from the dynamic shear modulus tests at 10 rad/s conducted in the linear viscoelastic range on binder specimens at different aging levels, i.e., unaged, aging conditioned using the RTFO, and aging conditioned using the PAV after the RTFO conditioning. For the unaged and RTFO-aged specimens, the temperature sweep shear modulus test started at 40 °C and 46 °C, respectively, and the testing temperature increased with a 6 °C increment according to AASHTO M 320. Two replicates were tested at each aging condition.

The MSCR test was conducted on the specimens after the RTFO aging conditioning as per AASHTO T 350. The test was performed by applying creep stresses with two magnitudes, i.e., 0.1 and 3.2 kPa at 52 and 58 °C. Two parameters were obtained from the MSCR test, i.e., the non-recoverable creep compliance, $J_{nr}$, and the percent recovery, $R$. The recovery percent at creep stress levels of 0.1 and 3.2 kPa ($R_{0.1}$ and $R_{3.2}$) were calculated using Equations (4) and (5), respectively.

$$R_{0.1} = \frac{\sum_{N=11}^{20}[\in_{r(0.1,N)}]}{10} \quad (4)$$

$$R_{3.2} = \frac{\sum_{N=1}^{10}[\in_{r(3.2,N)}]}{10} \quad (5)$$

where $N$ is the cycle number at each stress level and $\in_r$ is the percent recovery at 0.1 kPa and 3.2 kPa. The non-recoverable compliance was calculated by the Eqs. (6) and (7), and the percent difference in non-recoverable creep compliance could then be expressed as Eq. (8).

$$J_{nr_{0.1}} = \frac{\sum_{N=11}^{20}[J_{nr(0.1,N)}]}{10} \quad (6)$$

$$J_{nr_{3.2}} = \frac{\sum_{N=1}^{10}[J_{nr(3.2,N)}]}{10} \quad (7)$$

$$J_{nr_{diff}} = \frac{[J_{nr_{3.2}} - J_{nr_{0.1}}] \times 100}{J_{nr_{0.1}}} \quad (8)$$

### 3.4. Intermediate-Temperature tests for cracking resistance evaluation

In this study, the cracking potentials of the asphalt binders were assessed using the Glover-Rowe parameter and the fatigue performance predicted using the LAS tests and the ViscoElastic Continuum Damage (VECD) model.

The G-R parameter was calculated using the dynamic shear modulus data at 0.005 rad/s and 15 °C. The parameter was developed as a rheological index to evaluate the fatigue cracking resistance of asphalt binders at low temperatures [19,20]. The parameter was defined as presented in Eq. (9):

$$G - R = \frac{G^* \cos^2\delta}{\sin\delta} \quad (9)$$

where $G^*$ is the complex shear modulus and $\delta$ is the phase angle at the corresponding temperature and loading frequency. The thresholds for the damage onset and the significant cracking were 180 kPa and 450 kPa, respectively.

The LAS test was conducted to evaluate the binder fatigue resistance and predict its fatigue life under repeated loads as per AASHTO T 391. The test was performed using the DSR with 8 mm-diameter plates at 16 °C on specimens after the RTFO and PAV aging conditioning. Prior to the LAS test, a frequency sweep test at frequencies from 0.2 to 30 Hz with constant strain level of 0.1% was performed to obtain the undamaged material properties within the linear viscoelastic range. The LAS test was then conducted at a frequency of 10 Hz with increasing shear strain from zero to 30% over 3100 cycles of loading. The VECD model was used to analyze the testing results. According to the LAS testing protocol, the definition of failure was 35% reduction in modulus, or, in other words, when the material integrity, $C$, defined by Equation (10), decreased from the value of 1 to 0.65.

$$C(t) = \frac{|G^*|(t)}{|G^*|_{initial}} \quad (10)$$

where $|G^*|(t)$ is the complex modulus at time $t$, and $|G^*|_{\text{initial}}$ is the undamaged and initial value of $|G^*|$. The number of cycles to failure can be calculated by Eq. (11).

$$N_f = A(\gamma_{\max})^B \quad (11)$$

where $N_f$ is fatigue life, $\gamma_{\max}$ is the maximum shear strain for the pavement structure, and $A$ and $B$ are the model coefficients.

### 3.5. Thermal behavior evaluation

In addition to enhancing the binder low-temperature performance, another merit of using PCM is to improve materials' thermal behavior. PCM can absorb extensive amount of heat at temperatures close to their

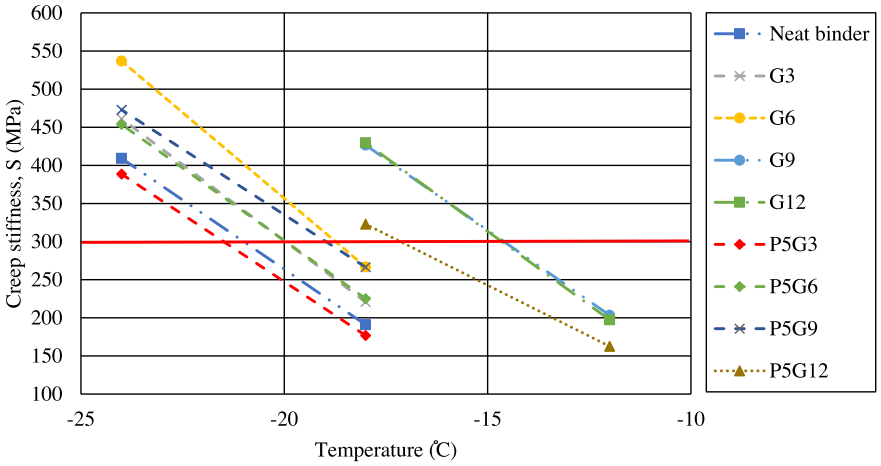


(a)

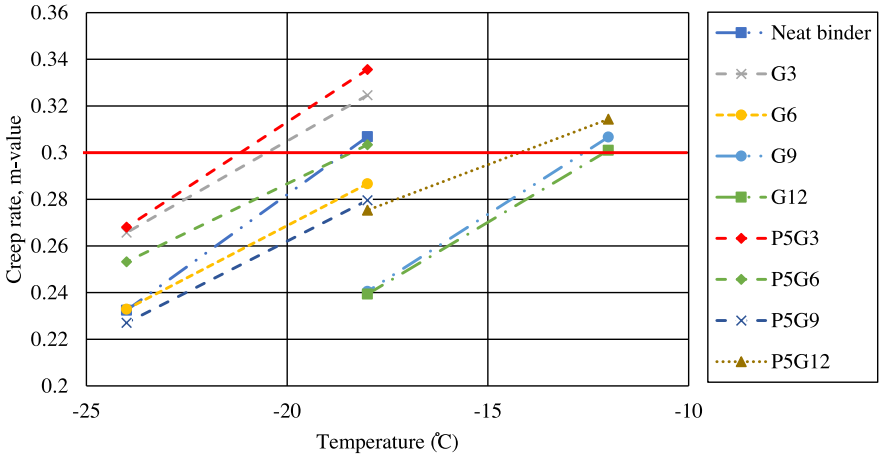


(b)

**Fig. 1.** Low-temperature performance of neat and modified binders, (a) creep stiffness value, and (b) m-value.

melting point and, thus, mitigate the temperature changes within the asphalt mixtures. In this study, two important thermal properties of the asphalt binders, i.e., the thermal conductivity and volumetric heat capacity were first measured using the Thermal Constants Analyzer (TPS 500S, Hot Disk, Sweden). The specimens were prepared as pellets and tested at room temperature of 21 ± 1 °C.

In addition, the thermogravimetric analysis (TGA) was performed to evaluate the thermal stability of the binders. In this test, the decomposition temperature was analyzed using the TGA and Differential Thermal Analysis (DTG) curves. During the test, binders with a mass of around 10 mg were heated from room temperature to 800 °C under nitrogen atmosphere flow. The heating rate was set at 10 °C/min.

To complete a full evaluation of the thermal properties of the modified binder, the researchers also used a Differential Scanning Calorimetry (DSC) to measure the glass transition temperature. The glass transition was defined as a reversible change of material from the viscoelastic state to the glassy or brittle state [21], and during the transition, the molecular motions were immobilized. Below the glass

**Table 5**
Binder Codes, Composition, and Low-temperature Performance Grade of Binders.

| Binder | Critical temperature by creep stiffness (°C) | Critical temperature by m-value (°C) | *S* or m-value controlled | Critical Temperature (°C) by *S* and m-value | Low PG | $\Delta T_c$ |
|---|---|---|---|---|---|---|
| Neat binder | −21 | −18.5 | m-value controlled | −18.5 | −28 | −2.5 |
| G3 | −20 | −18.3 | m-value controlled | −18.3 | −28 | −1.7 |
| G6 | −18.7 | −16.5 | m-value controlled | −16.5 | −22 | −2.2 |
| G9 | −14.6 | −12.6 | m-value controlled | −12.6 | −22 | −2 |
| G12 | −14.6 | −12.1 | m-value controlled | −12.1 | −22 | −2.5 |
| P5G3 | −21.5 | −21.0 | m-value controlled | −21 | −28 | −0.5 |
| P5G6 | −19.9 | −18.3 | m-value controlled | −18.3 | −28 | −1.6 |
| P5G9 | −19.0 | −15.7 | m-value controlled | −15.7 | −22 | −3.3 |
| P5G12 | −17.8 | −14.2 | m-value controlled | −14.2 | −22 | −3.6 |

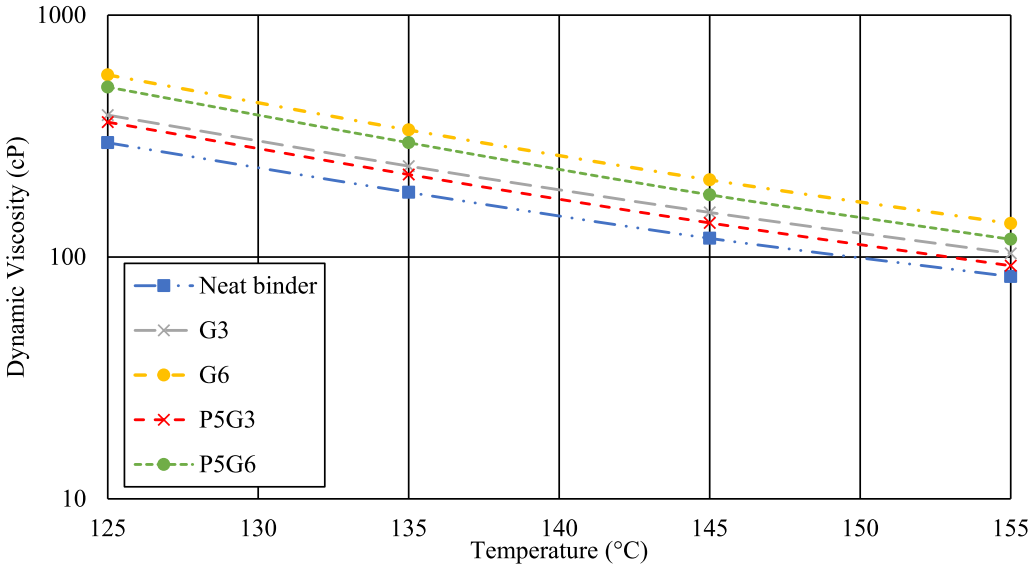


**Fig. 2.** Dynamic shear viscosity at different temperatures.

transition temperature, asphalt binder exhibited glassy and brittle behaviors, and at temperatures above the glass transition temperature, viscoelasticity dominated the material behaviors [22]. In this study, the DSC scan was conducted from −60 °C to 100 °C at a heating rate of 2 °C/min under nitrogen atmosphere flow.

## 4. Testing results

### 4.1. Binder performance evaluations

#### 4.1.1. Low-temperature performance of the Gilsonite-PCM-modified binders

While the dosage of PEG was fixed at 5% to prevent segregation, the low-temperature performance of the binders with different gilsonite contents were evaluated using the BBR creep stiffness tests. Fig. 1 illustrates the creep stiffness and the m-values for the neat and modified binders. The critical temperatures for creep stiffness, $S$, and creep rate, $m$, were determined at threshold values at 300 MPa, and 0.3, respectively, as indicated by the red lines. Table 5 summarizes the critical temperatures and the low performance grades of the binders with different concentration levels of modifiers. As the gilsonite content increased, the critical temperature increased, which indicates the adverse effects of gilsonite on the low-temperature performance of asphalt binders. At the same gilsonite concentration level, the critical temperature decreased by 2.4 °C in average with the addition of 5% PEG. As a result, the low PG of the G6 binder with PEG (P5G6) was restored from –22 to −28. Based on BBR testing results, the maximum gilsonite level was determined to be 6%, and in the remaining investigation, the binders with up to 6% gilsonite were tested.

The low temperature cracking resistance was further evaluated using the $\Delta T_c$ parameter. The parameter indicates the difference between the critical temperatures of creep stiffness and relaxation rate obtained from the BBR tests. If $\Delta T_c > 0$, the binder is stiffness-controlled or S-controlled; if $\Delta T_c < 0$, the binder is m value-controlled. An S-controlled binder or binder with higher $\Delta T_c$ values is usually more desirable. Table 5 presents the $\Delta T_c$ values of binders with different PEG and gilsonite contents. It can be observed that, for the P5G3 and P5G6 binders, the binders with PEG exhibited higher $\Delta T_c$ values than the ones with the same gilsonite concentration levels. The results showed that the addition of PEG improves the low temperature cracking resistance. For the P5G9 and P5G12 binders, the measured ΔTc values were lower than the ones of the binders without PEG. Because of their high value of low PG (i.e., –22) and low $\Delta T_c$, those two binders were not further evaluated in the study.

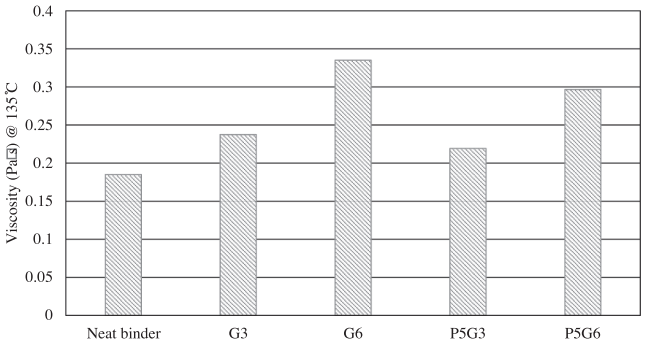


**Fig. 3.** The viscosity of samples at 135 °C.

#### 4.1.2. Evaluation of binder workability

After the performance evaluation, the workability of the modified binders was assessed using the rotational viscometer. Fig. 2 presents the dynamic shear viscosity curves at different temperatures for different binders. The testing results indicate that the gilsonite increased the viscosity of the binder and the addition of the PEG had moderated the viscosity of the binder at all temperatures. The binder viscosities are related to their workability. A low viscosity at the mixing and compaction temperature ranges can provide sufficient workability and potentially decrease the mixing and compaction temperature, which can lower the energy consumption and limit the greenhouse gas emissions [23]. The viscosity at the reference temperature of 135 °C was used as an index of the binder workability. Fig. 3 presents the viscosities of the binders at 135 °C. It can be observed that the binder with the gilsonite (G3 and G6) had high viscosity at 135 °C, and adding PEG to the gilsonite-modified binders decreased the binder viscosity and improved the workability. According to ASTM D6373, all the binders including G6 exhibited sufficient workability since their viscosities at 135 °C were lower than 3 Pa·s. Fig. 4 present the binder mixing and compaction temperatures based on the RV test results. The results indicate that the addition of 6% gilsonite increased the mixing and compaction temperatures by 10 °C compared with the neat binder; however, the mixing and compaction temperatures of the modified binders remained in the acceptable range.

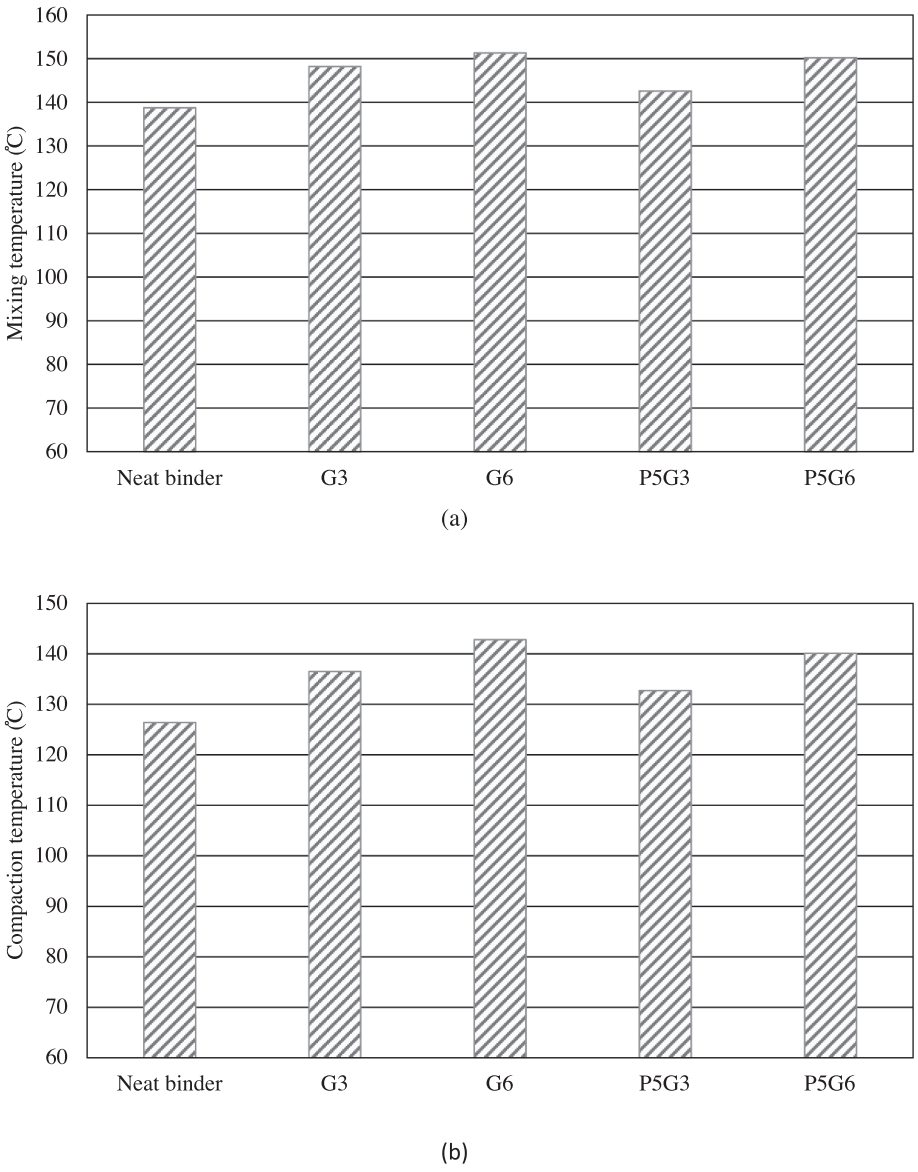


**Fig. 4.** (a) Average mixing temperature, (b) Average compaction temperature.

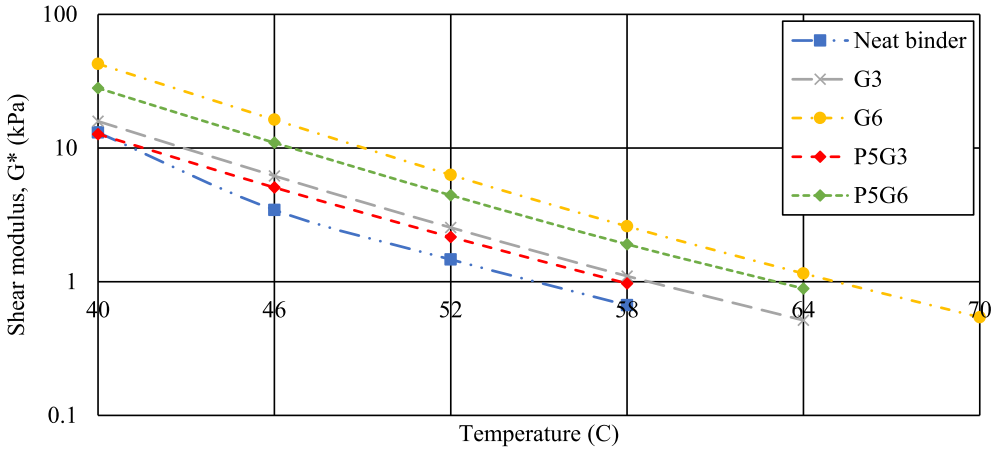


**Fig. 5.** Complex shear modulus of binders at different temperatures.

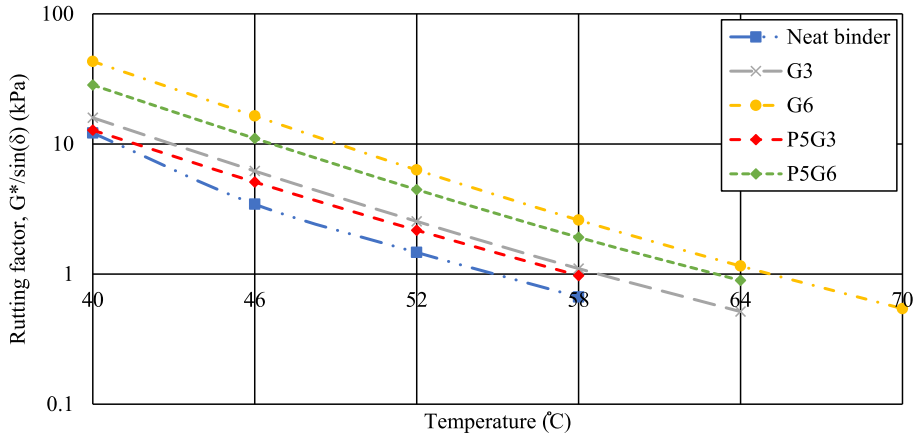


(a)

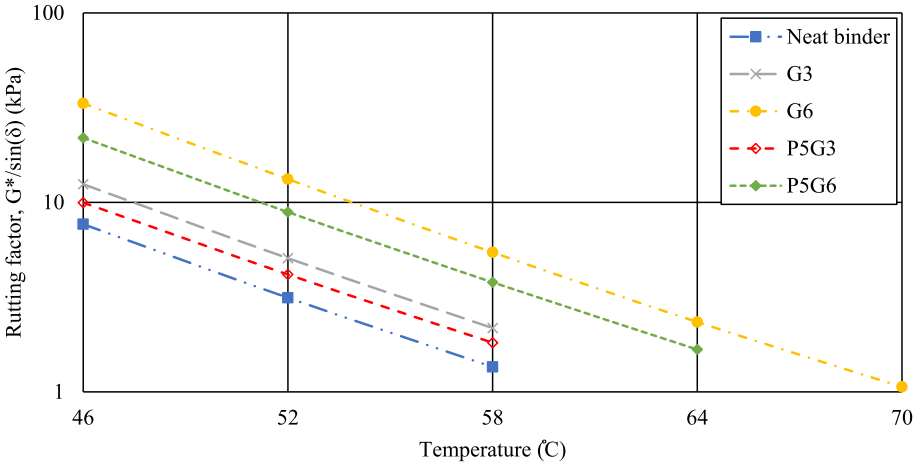


(b)

**Fig. 6.** Rutting factor of binders at different temperatures, (a) Unaged binder, (b) RTFO-aged binder.

**Table 6**
Critical Temperatures at Different Aging Conditions and Superpave Performance Grade (PG).

| Binder | Critical temperature (°C) | | | Superpave performance grade (PG) |
|---|---|---|---|---|
| | Unaged binder ($G^*/\sin\delta$) | RTFO aged binder ($G^*/\sin\delta$) | RTFO + PAV aged binder ($G^*\cdot\sin\delta$) | |
| Neat binder | 54.9 | 54.6 | 15.8 | 52–28 |
| G3 | 58.8 | 57.9 | 18.2 | 52–28 |
| G6 | 65.1 | 64.4 | 21.0 | 64–22 |
| P5G3 | 57.8 | 56.6 | 16.0 | 52–28 |
| P5G6 | 63.1 | 62.0 | 19.0 | 58–28 |

*4.1.3. High-temperature performance of the binders*

The high PG of the modified binders were tested through the dynamic shear modulus tests using a DSR. Fig. 5 presents the complex shear modulus curves of specimens at various temperatures tested at 10 Hz. It can be observed that as the concentration level of gilsonite increased, the shear modulus increased, and the addition of PEG also decreased the shear modulus at each temperature.

According to the Superpave PG grading specification AASHTO M 320, the rutting factor ($G^*/\sin\delta$) reflects the rutting resistance of the asphalt binder. A higher $G^*/\sin\delta$ value indicates greater rutting resistance. In Fig. 6, the G3 and G6 binders exhibited higher $G^*/\sin\delta$ values than the neat binder. The addition of PEG decreased the $G^*/\sin\delta$ values at each gilsonite concentration level. According to Superpave specification, the rutting factor should be at least 1.00 kPa before RTFO aging and 2.2 kPa after RTFO short-term aging conditioning. The critical temperatures to pass the rutting criteria and the high PGs of the binders are presented in Table 6. The testing results indicated that the addition of 6% gilsonite (G6) increased the high PG by two levels from PG 52 to 64. The addition of the 5% PEG balanced the performance at the high and low temperatures and lowered the high PG by one grade at each gilsonite concentration level. Moreover, though the G6 binder is one level higher than that of the P5G6 binder, the critical temperatures for

**Table 7**
R, Jnr, and $J_{nr,diff}$ of the Neat Binder and Modified Binders.

| Binder specimen | Temperature (°C) | $J_{nr}$ (kPa$^{-1}$) | | Recovery (%) | | $J_{nr,diff}$ (%) |
|---|---|---|---|---|---|---|
| | | 0.1 kPa | 3.2 kPa | 0.1 kPa | 3.2 kPa | |
| Neat binder | 52 | 2.72 | 3.09 | 2.96 | 0 | 13.59 |
| | 58 | 6.54 | 7.34 | 0.33 | 0 | 12.24 |
| G3 | 52 | 1.68 | 1.86 | 4.42 | 0.49 | 10.70 |
| | 58 | 4.16 | 4.53 | 0.90 | 0 | 8.73 |
| G6 | 52 | 0.57 | 0.63 | 11.57 | 5.43 | 10.88 |
| | 58 | 1.51 | 1.71 | 6.12 | 0.86 | 13.23 |
| P5G3 | 52 | 1.95 | 2.43 | 4.81 | 1.02 | 24.21 |
| | 58 | 4.79 | 5.95 | 1.52 | 0 | 24.20 |
| P5G6 | 52 | 0.78 | 0.94 | 13.52 | 6.34 | 21.50 |
| | 58 | 2.04 | 2.64 | 7.64 | 0.72 | 29.15 |

the unaged and the RTFO aged binder are only 2 °C and 2.4 °C lower than those of the G6 binder, respectively, and they are higher than those of the neat binder by 8.2 °C and 7.4 °C, respectively. With the addition of PEG and gilsonite, the P5G6 binder is almost qualified to be PG 64–28. The intermediate critical temperatures determined by the cracking factor $G^*\cdot\sin\delta$ are also presented in Table 6 for the purpose of performance grading.

#### 4.1.4. Multiple stress creep recovery (MSCR) test

In addition to the Superpave rutting factor, the rutting performance of the binders were evaluated beyond the linear viscoelastic range using the MSCR test on a DSR. The test was performed at 52 and 58 °C on specimens after RTFO aging conditioning. Table 7 and Fig. 7 present the average non-recoverable creep compliance ($J_{nr}$) at the stress levels of 0.1 and 3.2 kPa at 52 and 58 °C. Gilsonite-modified binders exhibited lower $J_{nr}$ values, which indicated a good performance of gilsonite against rutting. This trend could be observed from tests at both stress levels and both temperatures. Introducing PEG to gilsonite modified binder slightly increased the $J_{nr}$ values. Comparing the testing results from binders with different gilsonite concentration levels, it can be observed that the $J_{nr}$ values were dominated by the content of gilsonite. The modified binder P5G6 exhibited lower $J_{nr}$ at different temperatures than the G3 binder and the neat binder.

Recovery values ($R$) is another indicator of the rutting resistance of the binders. A higher $R$ value indicates more elastic recovery after loading. According to Table 7, while the elastic recovery of the neat binder at 3.2 kPa was found as zero, after adding 6% gilsonite, the $R$ value was increased to 6.34%. Table 7 and Fig. 8 also indicate that the $R$ values of the P5G6 and G6 binder were significantly higher than binders with other gilsonite concentration level. Unlike the trend in $J_{nr}$, the addition of 5% PEG slightly increased the $R$ value at each gilsonite concentration level. The MSCR testing standard requires the difference

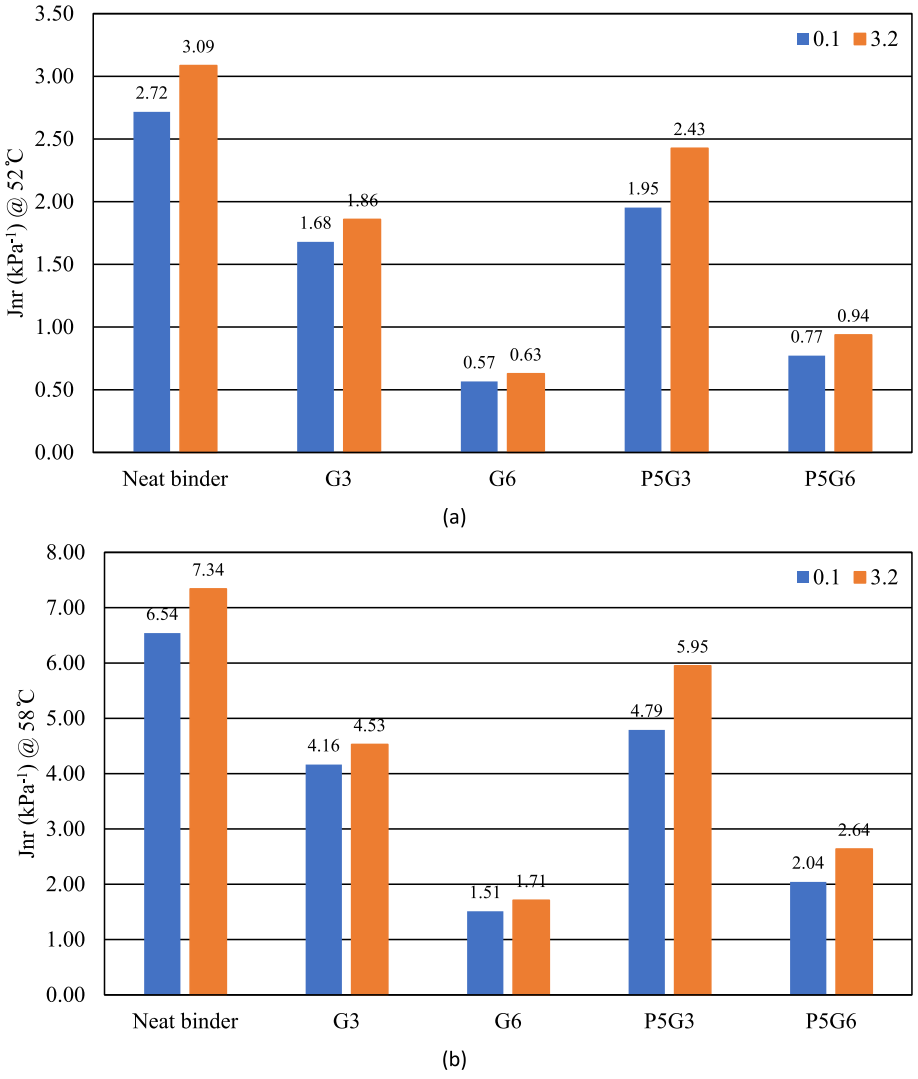


**Fig. 7.** Non-recoverable creep compliance at (a) 52 °C, (b) 58 °C.

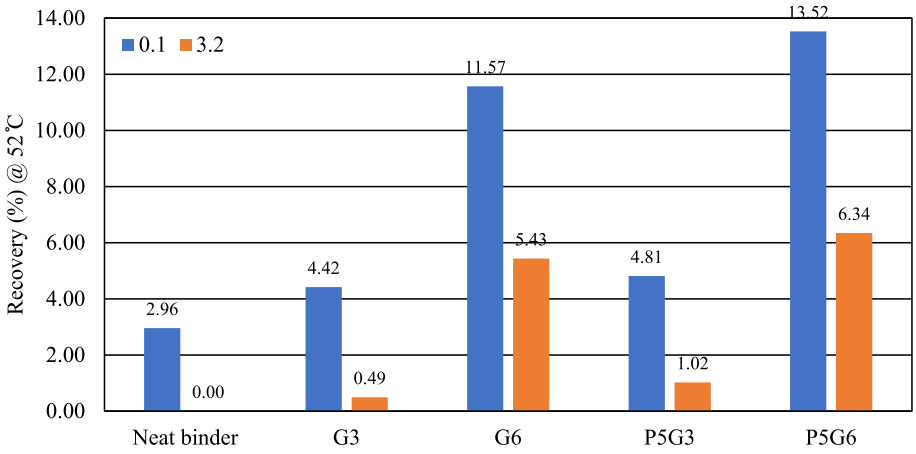


(a)

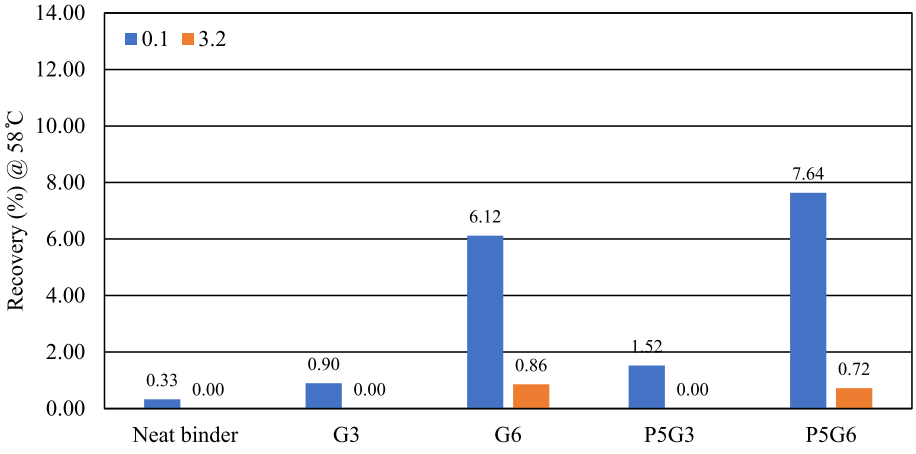


(b)

**Fig. 8.** Percent recovery at (a) 52 °C, (b) 58 °C.

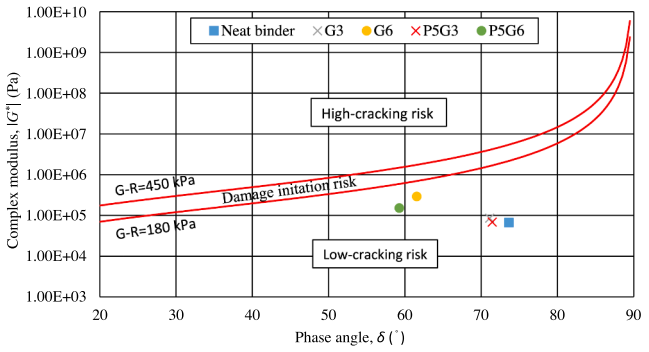


**Fig. 9.** Average values of the G-R parameter for the neat binder and modified binders.

between the creep compliance at 3.2 kPa and 0.1 kPa to 75% and no binder exceeded the 75% limit.

In summary, both the rutting factor $G^*/\sin\delta$ and the MSCR test results indicated that the binders with 6% gilsonite (i.e., G6 and P5G6) exhibited superior rutting resistance and the addition of PEG has a minor impact of the rutting susceptibility at each gilsonite concentration level.

### 4.1.5. *Glover-Rowe parameter*

The Glover-Rowe (G-R) parameter was obtained from binder specimens after PAV aging conditioning to evaluate the binders' cracking resistance at intermediate temperatures. Fig. 9 presents the values of the G-R parameters of different binders in a Black diagram.

The results presented in Fig. 9 indicates that all the binders can pass the limit of cracking resistance based on the G-R parameters. However, the binders with 6% gilsonite had higher cracking potential than the ones with 3% or lower percentage of gilsonite. The G-R parameter also showed the addition of PEG to gilsonite-modified binders can decrease the risk of damage for 3% and 6% of gilsonite.

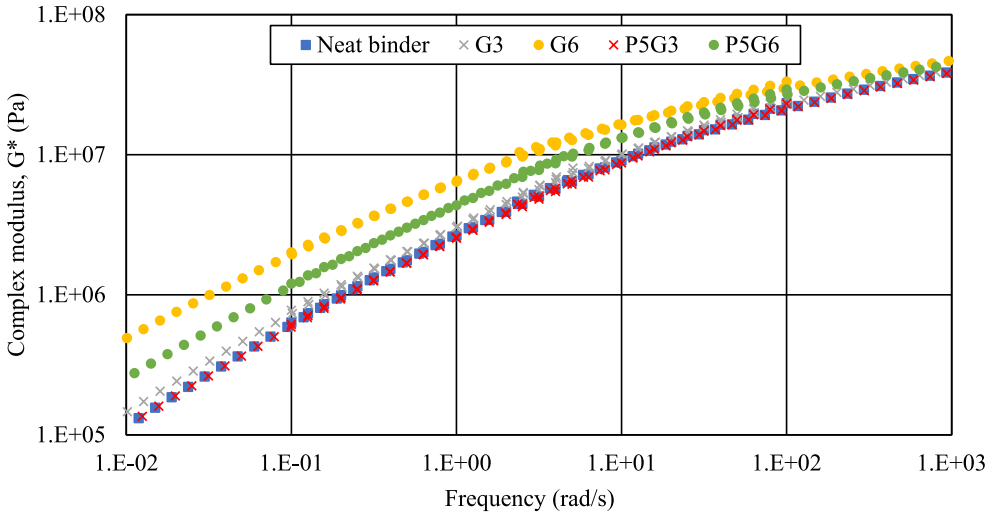


**Fig. 10.** Frequency sweep test of binders at 16 °C.

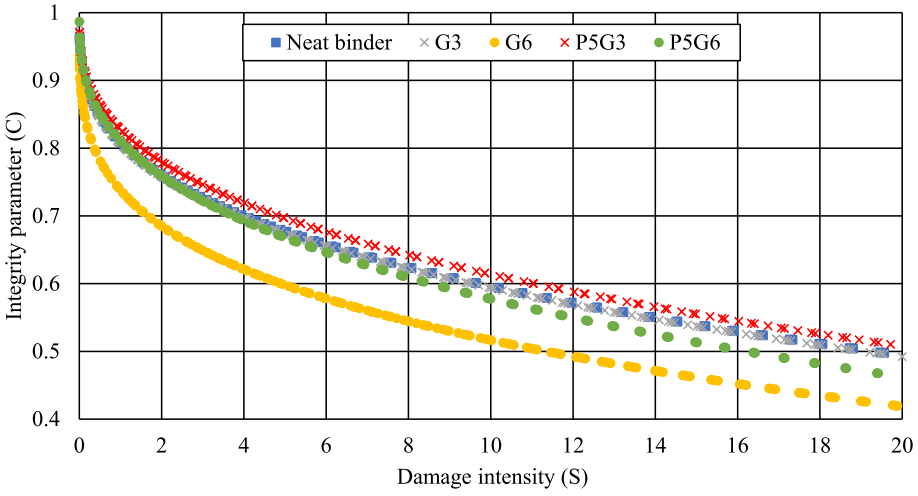


**Fig. 11.** Integrity parameter vs. damage intensity of binders.

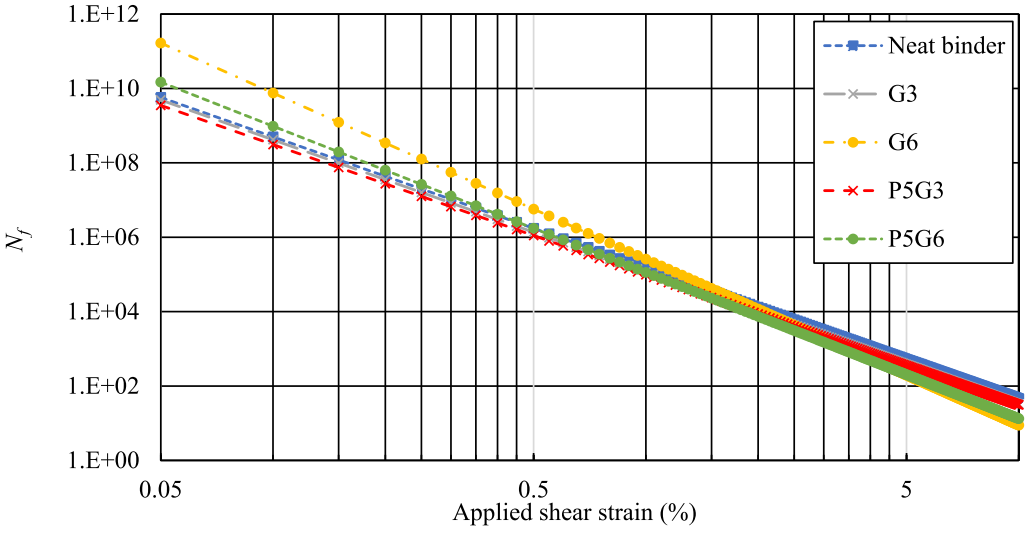


**Fig. 12.** Fatigue prediction model from the VECD model.

**Table 8**
Fatigue Parameters (A and B) and Fatigue Life at Different Strain Levels (1%, 2.5%, and 5.0%).

| Binder specimen | A | B | $N_f$ | | |
|---|---|---|---|---|---|
| | | | Strain level (1.0%) | Strain level (2.5%) | Strain level (5.0%) |
| Neat binder | 1.513E + 05 | −3.520 | 151,340 | 6,017 | 525 |
| G3 | 1.161E + 05 | −3.556 | 116,054 | 4,464 | 380 |
| G6 | 2.582E + 05 | −4.466 | 98,071 | 4,313 | 195 |
| P5G3 | 9.807E + 04 | −3.500 | 258,192 | 3,970 | 351 |
| P5G6 | 1.133E + 05 | −3.932 | 113,257 | 3,086 | 202 |

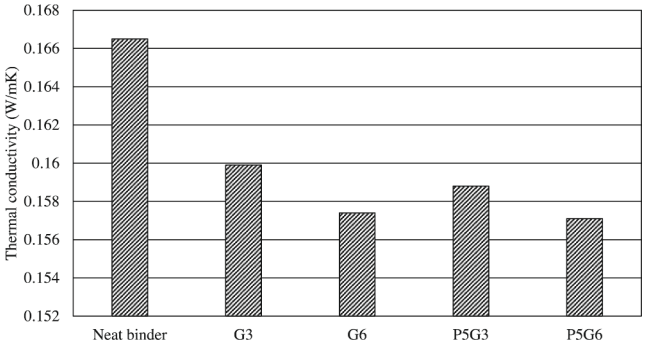


**Fig. 13.** Thermal conductivity of the neat binder and modified binders.

#### 4.1.6. Linear amplitude sweep (LAS) test

In addition to using the G-R parameters obtained from tests within the linear viscoelastic range, the LAS tests were performed to further assess the fatigue cracking resistance of the binders at intermediate temperatures. A frequency sweep "fingerprint" test was first conducted before each LAS test to quantify the linear viscoelastic properties of the binders. The results are presented in Fig. 10. Similar to complex modulus showed in Fig. 5, the testing results indicates that the binders with higher gilsonite content exhibited higher modulus and the addition of PEG can soften the binders at each gilsonite concentration level. Following the fingerprint test, the LAS test was performed. The damage characteristic curve obtained from the LAS test analyzed is one important component of the VECD model. The curve describes the relationship between material integrity ($C$) and the increase of the damage intensity ($S$). A higher C-S curve represents a lower deterioration rate and indicates a potential superior cracking resistance of the asphalt binders. In some recent studies, the ranking of the C-S curves has been reported to have high correlations with the ranking of the material stiffness [2425]. However, in this study, the testing results in Fig. 11 show that even though the G6 binder had the highest modulus, it had the lowest C-S curve or the highest integrity deterioration rate. The addition of PEG yielded higher C-S curve at each gilsonite concentration level, and the P5G3 binder had the highest C-S curve in this case.

Fig. 12 and Table 8 present the predicted numbers of cycles to failure for different binders at different strain levels. It can be observed that the binders with 6% gilsonite yielded $N_f$ vs. strain amplitude curves with high slopes, which means the fatigue lives of the G6 and P5G6 binders were greater than others at low strain amplitude levels and lower at high strain amplitudes. The addition of PEG increased the fatigue lives of the binders at each gilsonite concentration levels. The trend can also be observed from Table 8. At high strain levels, the fatigue lives of binders with 3% gilsonite were significantly higher than the binders with 6% gilsonite. However, the ranges of strains and stresses on asphalt binders may vary because of the local strain concentration. While the LAS tests predicted the fatigue lives of the binders at different strain levels, a fatigue evaluation on the mixture level in the future study would provide more information about the cracking resistance of those binders.

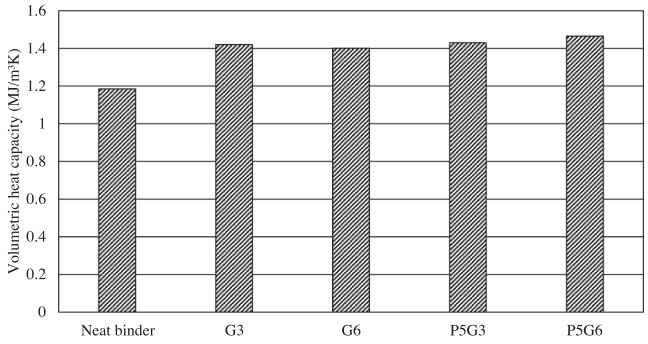


**Fig. 14.** Volumetric heat capacity of the neat binder and modified binders.

### 4.2. Thermal analysis

#### 4.2.1. Thermal conductivity and volumetric heat capacity

In addition to testing the rheological behaviors, the thermal conductivity and the volumetric heat capacity of the modified binders were measured in this study. The thermal conductivity and the volumetric heat capacity of the modified binders were measured in this study. A higher thermal conductivity leads to a quicker heat transfer through the asphalt pavement, which improves the thermoregulation of asphalt pavement and avoid the concentration of extreme temperature in the asphalt mixture [26]. Fig. 13 presents the measured thermal conductivity of the neat binder and modified binders. A descending trend in thermal conductivity was observed with the increase of gilsonite content, and the lowest thermal conductivity was observed in the sample P5G6. It also indicates that the addition of the PEG slightly decreases the thermal conductivity of gilsonite-modified binders. The lowest thermal conductivity was observed in the sample P5G6.

Another related thermal characteristic of asphalt mixture is volumetric heat capacity. A high volumetric heat capacity means the material can observe more energy while changing temperatures. For paving materials, greater values of volumetric heat capacity can mitigate the pavement temperature swing in pavements caused by the ambient temperature changes. Fig. 14 presents the volumetric heat capacity of the neat and modified binders. The testing results indicate the volumetric heat capacity was raised after the addition of gilsonite. Unlike the thermal conductivity results, the four gilsonite-modified binders had similar values of the volumetric heat capacity. The P5G6 binder had the highest volumetric heat among all the tested binders, 19.1% higher than the neat binder.

#### 4.2.2. Thermo-gravimetric analysis (TGA)

TGA is an effective test to monitor the mass loss with temperature changes to determine the thermal stability of binders by increasing temperature. Fig. 15 presents the weight losses of the samples as functions of temperature changes during the TGA tests. It can be observed that all the binders remained thermally stable before 250 °C. The neat binder first started to decompose as the temperature increased. At the same temperature, the neat binder had the most weight loss. The observation can be confirmed by the DTG curves presented in Fig. 16 which were obtained by calculating the first derivative of the weight loss over temperature. Furthermore, the single peak from the PEG-gilsonite-modified binders suggested that relatively strong molecular bonds existed among the PEG, gilsonite, and the neat binder, which led to the superior thermal stabilities of the modified binders.

#### 4.2.3. Differential scanning calorimetry (DSC) analysis

The heat flows of binders are presented in Fig. 17. It can be observed

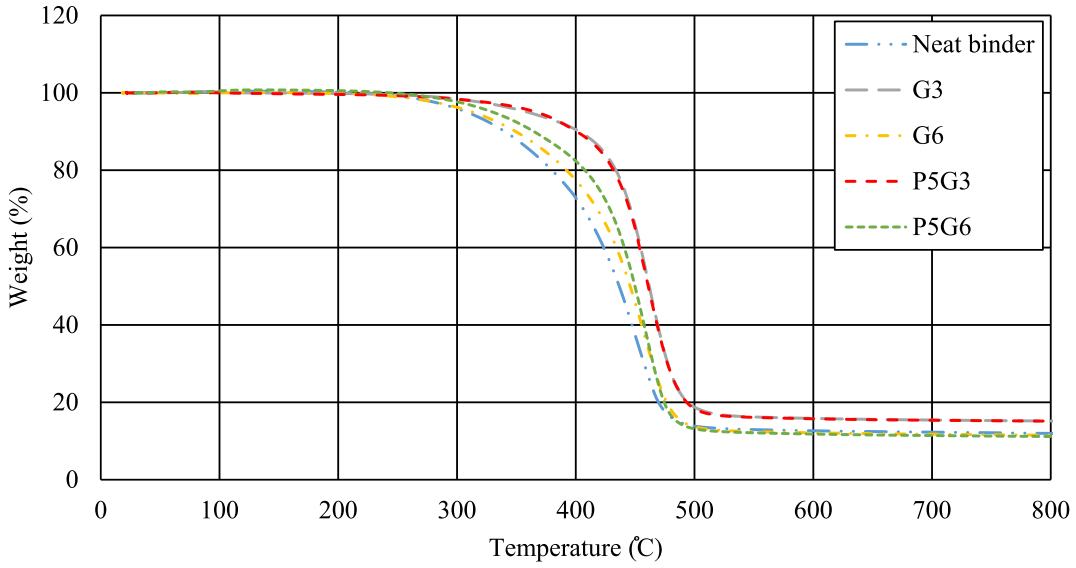


**Fig. 15.** TGA curves of the neat binder and modified binders.

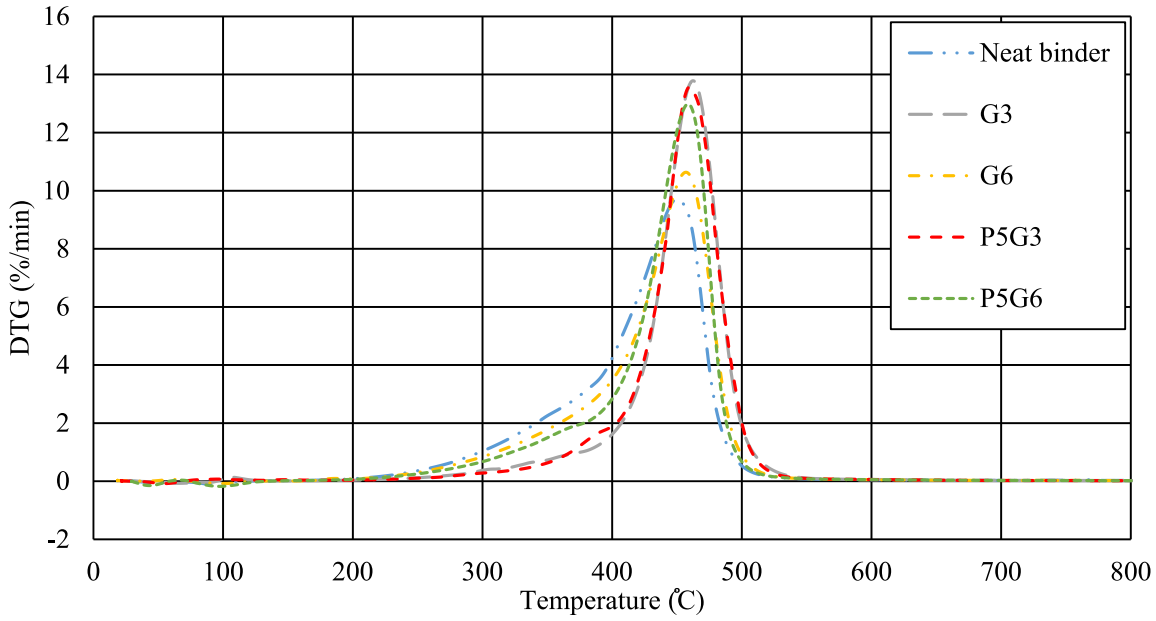


**Fig. 16.** DTG curves of the neat binder and modified binders.

that as the temperatures changed from low to high, the heat flows increased and reached to peak values around −30 °C for all binders. The temperatures corresponding to the peaks of heat flows were the glass transition temperatures. The values of the glass transition temperatures for different binders are presented in Fig. 18. The testing results indicate that the addition of PEG was able to lower the binder glass transition temperature and allowed the binder to remain viscoelastic and less brittle in a wider temperature range. As the dosage of gilsonite increased, the glass transition temperatures increased. The introduction of PEG mitigated the impact of gilsonite on the process of glass transitions. For example, with 6% gilsonite, the transition temperature was raised from −28.7 °C, the temperature of neat binder, to −24.9 °C. With 5% PEG, the glass transition temperature was improved to −26.2 °C. Based on molecular theory, there are two main factors affecting the glass transition temperatures, i.e., the force between the polymer molecules and the flexibility of molecule chains. It was believed that the addition of PEG increased the flexibility of the molecular chains; thus, lowered the glass transition temperatures and expanded the temperature range for the material to remain viscoelastic.

## 5. Conclusions and future work

The objective of the study was to evaluate the impact of PCM on the rheological and thermal behaviors of the gilsonite-modified binder and identify the proper dosages of PCM and gilsonite so that the binder high-temperature performance can be improved without sacrificing the low-temperature performance. The performance test and thermal analysis results indicated that the G3 and P5G6 binders managed to increase the high PG of the original binder by one grade without increasing the low PG. The MSCR test results showed that even though the G3 and P5G6 binders had the same high PG, P5G6 had much lower non-recovery creep compliance and higher percentage recovery under the same loading scenarios; thus, having superior rutting resistance at high temperatures.

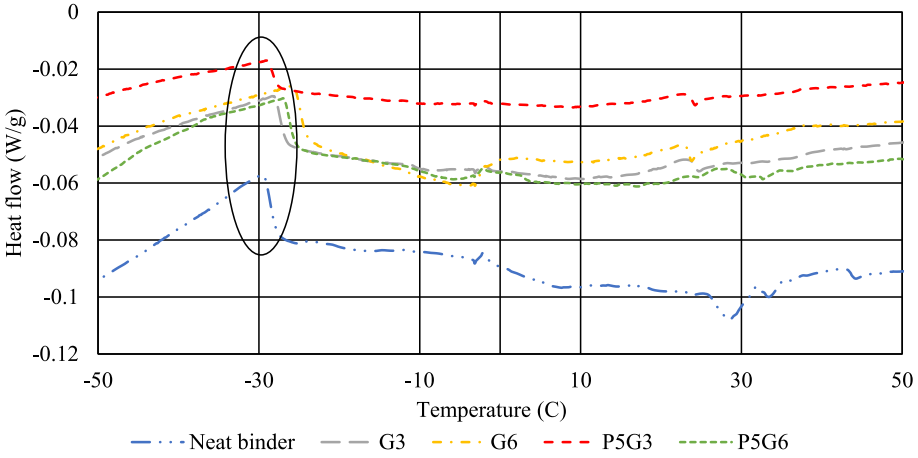


**Fig. 17.** DSC curves of the neat binder and modified binders.

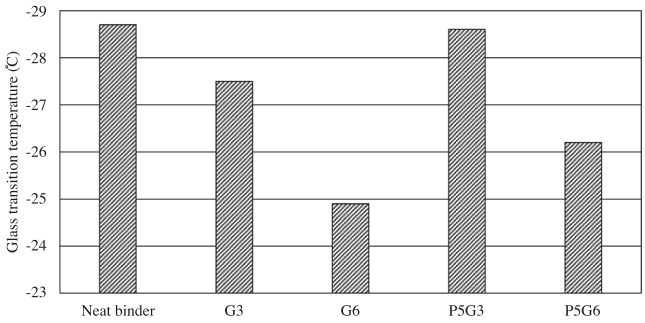


**Fig. 18.** Glass transition temperature of the neat binder and modified binders.

Other major findings are highlighted and presented in the following:

- Gilsonite improves the high-temperature performance of asphalt binders and has adverse effects on their performance at low temperatures. With 5% PEG incorporated, binder with Gilsonite up to 6% was able to remain the same low PG as the neat binder. As for the continuous PG, the high PG of the P5G6 binder reached 63, nearly two levels higher than the original binder.
- In addition to the Superpave performance grading tests, the MSCR and the LAS tests were conducted to assess the modified binders' rutting and cracking resistance, respectively. The MSCR tests verified the findings in the Superpave rutting tests and clearly showed that the P5G6 binder had superior rutting resistance. On the other hand, the LAS fatigue test and the VECD analysis results indicated that the binders with 6% Gilsonite without PEG were stiffer and could yield longer fatigue life at low loading amplitudes and fewer numbers of cycles to failure with high loading amplitudes. Asphalt mixture tests were recommended for further fatigue cracking resistance evaluation.
- Thermal analysis suggested that the volumetric heat capacity of the gilsonite-modified and the PEG-gilsonite-modified binders were significantly higher than the virgin binder, which can improve the thermoregulation of asphalt binder.

For future studies, it is recommended that base binders with different PGs and sources be tested with the recommend dosages of PEG and Gilsonite to verify the findings from this study. The cost-benefit analysis will be conducted. Furthermore, performance tests and thermal behavior analyses can be performed on the corresponding asphalt mixtures in the future.

## CRediT authorship contribution statement

**K. Farshad Saberi:** Writing – original draft, Methodology, Investigation, Formal analysis, Data curation, Conceptualization. **Yizhuang David Wang:** Writing – review & editing, Writing – original draft, Supervision, Project administration, Methodology, Investigation, Formal analysis, Conceptualization. **Jenny Liu:** Supervision, Project administration, Funding acquisition, Conceptualization, Investigation, Methodology, Writing – review & editing.

## Declaration of Competing Interest

The authors declare that they have no known competing financial interests or personal relationships that could have appeared to influence the work reported in this paper.

## Data availability

Data will be made available on request.

## Acknowledgement

The authors acknowledge the National Center for Transportation Infrastructure Durability & Life-Extension, U. S. Department of Transportation for funding this research under the grant 2020-MST-02. The authors also appreciate the material supplier AMERICAN GILSONITE COMPANY for their support and providing Gilsonite samples for conducting this research.

## References

[1] J. Liu, P. Li, Experimental study on gilsonite-modified asphalt, Airfield Highway Pavements (2008).
[2] D. Mirzaiyan, M. Ameri, A. Amini, M. Sabouri, A. Norouzi, Evaluation of the performance and temperature susceptibility of gilsonite- and SBS-modified asphalt binders, Constr. Build. Mater. 207 (2019) 679–692, https://doi.org/10.1016/j.conbuildmat.2019.02.145.
[3] M. Ameri, A. Mansourian, S.S. Ashani, G. Yadollahi, Technical study on the Iranian Gilsonite as an additive for modification of asphalt binders used in pavement construction, Constr. Build. Mater. 25 (3) (2011) 1379–1387, https://doi.org/10.1016/j.conbuildmat.2010.09.005.
[4] S. Ren, M. Liang, W. Fan, Y. Zhang, C. Qian, Y. He, J. Shi, Investigating the effects of SBR on the properties of gilsonite modified asphalt, Constr. Build. Mater. 190 (2018) 1103–1116.
[5] M. Ameri, A. Mansourian, A.H. Sheikhmotevali, Investigating effects of ethylene vinyl acetate and gilsonite modifiers upon performance of base bitumen using Superpave tests methodology, Constr. Build. Mater. 36 (2012) 1001–1007, https://doi.org/10.1016/j.conbuildmat.2012.04.137.
[6] M. Ameri, D. Mirzaiyan, A. Amini, Rutting resistance and fatigue behavior of gilsonite-modified asphalt binders, J. Mater. Civ. Eng. 30 (11) (2018) 04018292, https://doi.org/10.1061/(asce)mt.1943-5533.0002468.

[7] H.A.R. Quintana, J.A.H. Noguera, C.F.U. Bonells, Behavior of gilsonite-modified hot mix asphalt by wet and dry processes, J. Mater. Civ. Eng. 28 (2) (2016) 04015114, https://doi.org/10.1061/(asce)mt.1943-5533.0001339.
[8] S. Aflaki, N. Tabatabaee, Proposals for modification of Iranian bitumen to meet the climatic requirements of Iran, Constr. Build. Mater. 23 (6) (2009) 2141–2150, https://doi.org/10.1016/j.conbuildmat.2008.12.014.
[9] M.H. Sehhat, A. Mahdianikhotbesara, Powder spreading in laser-powder bed fusion process, Granul. Matter 23 (4) (2021) 1–18, https://doi.org/10.1007/s10035-021-01162-x.
[10] B.V. Kök, M. Yilmaz, M. Guler, Evaluation of high temperature performance of SBS + Gilsonite modified binder, Fuel 90 (10) (2011) 3093–3099, https://doi.org/10.1016/j.fuel.2011.05.021.
[11] Y. Zhang, G. Zhou, K. Lin, Q. Zhang, H. Di, Application of latent heat thermal energy storage in buildings: state-of-the-art and outlook, Build. Environ. 42 (6) (2007) 2197–2209, https://doi.org/10.1016/j.buildenv.2006.07.023.
[12] H. Zhang, X. Wang, D. Wu, Silica encapsulation of n-octadecane via sol-gel process: a novel microencapsulated phase-change material with enhanced thermal conductivity and performance, J. Colloid Interface Sci. 343 (1) (2010) 246–255, https://doi.org/10.1016/j.jcis.2009.11.036.
[13] Y. Farnam, H.S. Esmaeeli, P.D. Zavattieri, J. Haddock, J. Weiss, Incorporating phase change materials in concrete pavement to melt snow and ice, Cem. Concr. Compos. 84 (2017) 134–145, https://doi.org/10.1016/j.cemconcomp.2017.09.002.
[14] Z. Lei, H. Bahia, T. Yi-Qiu, Effect of bio-based and refined waste oil modifiers on low temperature performance of asphalt binders, Constr. Build. Mater. 86 (2015) 95–100, https://doi.org/10.1016/j.conbuildmat.2015.03.106.
[15] P. Kriz, J. Stastna, L. Zanzotto, Glass transition and phase stability in asphalt binders, Road Mater. Pavement Design 9 (sup1) (2008) 37–65.
[16] M. Guo, M. Liang, Y. Fu, A. Sreeram, A. Bhasin, Average molecular structure models of unaged asphalt binder fractions, Mater. Struct. Vol. 54, Iss. 173 (2021), https://doi.org/10.1617/s11527-021-01754-2.
[17] M.R. Kakar, Z. Refaa, J. Worlitschek, A. Stamatiou, M.N. Partl, M. Bueno, Thermal and rheological characterization of bitumen modified with microencapsulated phase change materials, Constr. Build. Mater. 215 (2019) 171–179, https://doi.org/10.1016/j.conbuildmat.2019.04.171.
[18] K. Wei, X. Wang, B. Ma, W. Shi, S. Duan, F. Liu, Study on rheological properties and phase-change temperature control of asphalt modified by polyurethane solid–solid phase change material, Sol. Energy 194 (November) (2019) 893–902, https://doi.org/10.1016/j.solener.2019.11.007.
[19] G.M. Rowe, G. King, M. Anderson, The influence of binder rheology on the cracking of asphalt mixes in airport and highway projects, J. Test. Eval. 42 (5) (2014) pp, https://doi.org/10.1520/JTE20130245.
[20] F. Moreno-Navarro, M. Sol-Sánchez, F. Gámiz, M.C. Rubio-Gámez, Mechanical and thermal properties of graphene modified asphalt binders, Constr. Build. Mater. 180 (2018) 265–274, https://doi.org/10.1016/j.conbuildmat.2018.05.259.
[21] T. Wang, F. Xiao, S. Amirkhanian, W. Huang, M. Zheng, A review on low temperature performances of rubberized asphalt materials, Constr. Build. Mater. 145 (Aug. 2017) 483–505, https://doi.org/10.1016/j.conbuildmat.2017.04.031.
[22] N. Baldino, D. Gabriele, C.O. Rossi, L. Seta, F.R. Lupi, P. Caputo, Low temperature rheology of polyphosphoric acid (PPA) added bitumen, Constr. Build. Mater. 36 (2012) 592–596, https://doi.org/10.1016/j.conbuildmat.2012.06.011.
[23] Z. Sun, J. Yi, Y. Huang, D. Feng, C. Guo, Properties of asphalt binder modified by bio-oil derived from waste cooking oil, Constr. Build. Mater. 102 (Jan. 2016) 496–504, https://doi.org/10.1016/j.conbuildmat.2015.10.173.
[24] Y. Wang, Y. Richard Kim, Development of a pseudo strain energy-based fatigue failure criterion for asphalt mixtures, Int. J. Pavement Eng. 20 (10) (2019) 1182–1192, https://doi.org/10.1080/10298436.2017.1394100.
[25] Y.D. Wang, B.S. Underwood, Y.R. Kim, Development of a fatigue index parameter, Sapp, for asphalt mixes using viscoelastic continuum damage theory, Int. J. Pavement Eng. 23 (2) (2022) 438–452.
[26] P. Pan, S. Wu, Y. Xiao, P. Wang, X. Liu, Influence of graphite on the thermal characteristics and anti-ageing properties of asphalt binder, Constr. Build. Mater. 68 (2014) 220–226, https://doi.org/10.1016/j.conbuildmat.2014.06.069.